

# Self-organized network design by link survivals and shortcuts

Yukio Hayashi<sup>a</sup>, Yuki Meguro<sup>a</sup>

<sup>a</sup>*Japan Advanced Institute of Science and Technology, Ishikawa 923-1292, Japan*

---

## Abstract

One of the challenges for future infrastructures is how to design a network with high efficiency and strong connectivity at low cost. We propose self-organized geographical networks beyond the vulnerable scale-free structure found in many real systems. The networks with spatially concentrated nodes emerge through link survival and path reinforcement on routing flows in a wireless environment with a constant transmission range of a node. In particular, we show that adding some shortcuts induces both the small-world effect and a significant improvement of the robustness to the same level as in the optimal bimodal networks. Such a simple universal mechanism will open prospective ways for several applications in wide-area ad hoc networks, smart grids, and urban planning.

*Key words:* Complex network science; Geographical networks; Population density; Unit disk graph; Decentralized routing

*PACS:* 89.75.Fb, 89.20.Ff, 89.40.-a, 05.65.+b

---

## 1 Introduction

The self-organization of a network appears in a variety of subjects: biological growth, river formation, urban planning, and technological infrastructure design. They are too diverse to comprehend the complex processes involved in chemical, physical, and socioeconomic phenomena. While we do not insist on the detailed processes, we may find a common mechanism for generating efficient and robust networks at low cost in an optimization principle. In particular, a point of contact in the fields of biology, computer science, and physics is important for understanding a foundation for the self-organization mechanism.

Some biologically-motivated algorithms may be useful, e.g., the slime mold *Physarum polycephalum* forms efficient, economic, and fault-tolerant networks

similar to the railway system in the Tokyo metropolitan area [1]. In the networks, each node tends to connect to neighbor nodes in order to approach food sources, and some links which do not contribute to energy transport gradually disappear. Thus, short paths between any two nodes are self-organized on a planar space. A similar mechanism based on diffusive growth following chemotaxis is applied in the modeling of leaf venation patterns [2] and morphogenesis [3,4]. Moreover, in human trail systems [5], frequently used trails are more strongly marked, but rarely used trails are destroyed by the weathering effect. Apart from detailed processes, the key concepts of self-organization are the selective reinforcement of preferred routes and the removal of redundant connections. Removing the weakest links is also economically reasonable in the natural selection for maintaining efficient transportation and communication networks [6].

In complex network science, several models have been proposed for the coevolution of network formation and opinion spreading with the phase transition of the community size [7,8] and for the coupled dynamics with network evolution and packet flows by random walkers [9,10]; the hub emergence is parametrically controllable in the phase transition of the topological structure. Another idea of path reinforcement is introduced by iteratively adding a bypass between nodes separated by two hops on frequently traveled paths [11,12]. Through the induced diffusion process by random walkers, quasi-complete and scale-free (SF) networks emerge from the initial 1D-chain and 2D-lattice, respectively. However, in the topological formations involved with diffusive flow dynamics [7,8,9,10,11,12], the geographical positions of nodes are ignored or restricted in spite of their importance at least for transportation and communication networks. In addition, these network structures are not necessarily desirable due to the large cost of maintaining many links and the vulnerability against hub attacks [13].

On the other hand, a planar network emerges through directional growth just like in leaf venation patterns [2] for connecting to the geographical neighbors from new nodes whose positions follow a given spatial distribution related to the population density in city road formation [14]. It is also an attractive feature that in reaction-diffusion networks [15], various topologies, from homogeneous to heterogeneous structures, are controlled by rewirings according to the change of an external condition. In the typical model for ad hoc communication [16] related to adaptive linking mechanisms, a clustered network emerges on the random positions of nodes connected within a transmission range, in order to prevent energy consumption. Thus, beyond an extremely heterogeneous structure like SF networks, challenges to the self-organization of both efficient and robust networks are continued successfully.

In this paper, we aim to develop a new design method for the self-organization of networks in a wireless environment. The issues of connectivity, scalability,

routing and topology control in ad-hoc networks have been pointed out with the importance of mathematical models motivated by graph theory [16]. We further consider the strong effects of shortcuts on communication efficiency and the robustness of connectivity.

## 2 Network models

### 2.1 Initial configuration

Let us consider an initial network as a well-studied model for wireless ad hoc communication, which is called a unit disk graph (UDG) [16] in computer science. The decentralized complex system design is very important in challenging discussions for future network infrastructures [17]. Each node corresponds to a base station for multi-hop communication in a wireless environment. Without any biased condition, the positions of nodes are distributed uniformly at random in the normalized  $1.0 \times 1.0$  area. We assume that each node has a single transmission range denoted by  $A$ . In the disk area with the radius  $A/\sqrt{N_0}$  centered at a node, the node can directly communicate with its geographic neighboring nodes. Here,  $N_0$  is the network size (the total number of nodes) of a UDG. In other words, this condition for proximity connections is equivalent to  $d_{ij} < A/\sqrt{N_0}$ , where  $d_{ij}$  denotes the Euclidean distance between two nodes  $i$  and  $j$  on a plane, and  $1/\sqrt{N_0}$  is the normalization factor. Note that proximity connections are economically appropriate for transportation and communication networks, while low consumption for the transmission involves a weak connectivity. One of the issues related to the UDG is how large the transmission range needs to be connective between any nodes via a path of multi-hops in the networks.

Figure 1(a) shows the phase transition of the connectivity for a transmission range  $A$ . This result is consistent with that presented in Refs. [18,19]. We define the connectivity ratio by a relative size  $S/N_0$ ,  $S$  denotes the number of nodes which can reach each other via direct or multi-hop paths in the largest connected component (also called the giant component). In this paper, we use  $A = 2.0$  to be connective via a path between two nodes in almost all pairs. Although denser connections are obtained at each node for a larger value of  $A$ , it is numerically confirmed that our discussion is not affected by the results after this section. Because redundant links are removed in the course of time, even if there are many initial connections, then the remaining (not removed but surviving) links are almost the same as long as there is an initial high connectivity ratio. As shown in Fig. 1 (b), a UDG for  $A = 2.0$  consists of small degrees in the distribution with an exponential decay. Therefore, it has no hub, since the maximum degree is small as  $k_{max} \sim O(\log N_0)$  estimated

from  $\int_{k_{max}}^{\infty} P(k) \sim 1/N_0$ ,  $P(k) \sim e^{-\gamma k}$ , and  $\gamma > 0$ .

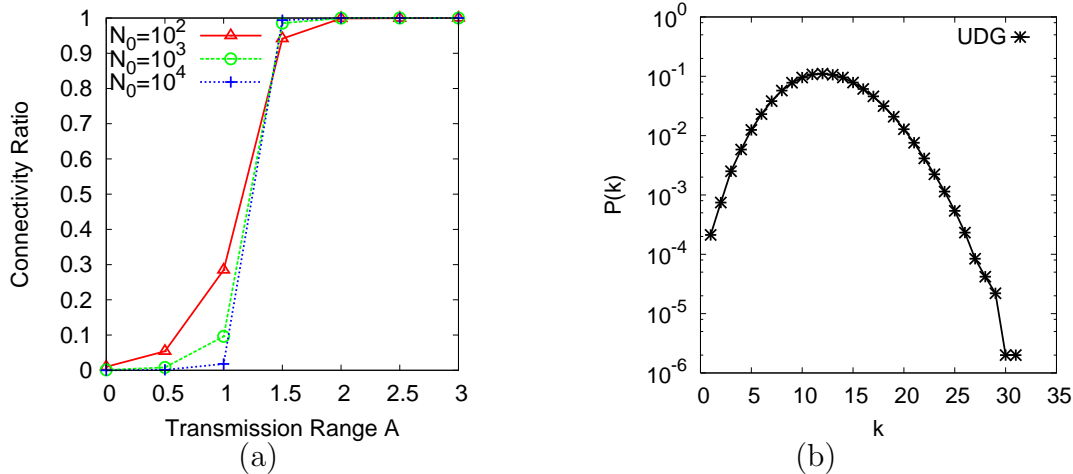


Fig. 1. (Color online) Basic property of the UDG. (a) Connectivity ratio vs. transmission range  $A$ . (b) Degree distribution in the UDG for  $A = 2.0$  and  $N_0 = 10000$ . Each value is obtained by the average of 50 realizations.

## 2.2 Communication request

At the beginning, to simplify the discussion, we consider only two types of nodes: the normal node and the active node corresponding to the food source [1]. We assume that the type is initially fixed at each node, for example, we set the number of active nodes are at 10% of the total  $N_0$ , and the remaining 90% are normal nodes. The positions of nodes are given by the UDG.

At each time step  $t$ ,  $R = 0.1N_t$  packets are generated over the network, where  $N_t$  is the number of surviving nodes at time  $t$ , as mentioned in Subsection 2.4. Some normal and active nodes are removed from the initial UDG in the self-organization of the network. Here, a communication request stochastically occurs between two nodes of the source and the terminal (where it is also called a destination in computer science) as follows: a packet is generated at rates  $p_n : p_a = 1 : 1000$  from normal and active source nodes. The terminal nodes are also randomly chosen at the rates. In other words, an active node is 1000 times more likely to be chosen as the source or terminal than a normal node<sup>1</sup>. Note that there is a one-to-one correspondence between source/terminal and packet. Thus, for  $R$  packets per step, the source and the terminal are randomly chosen for normal and active nodes according to the rates.

We can extend this simple setting of  $p_n$ ,  $p_a$ , and the fraction of nodes to any probability distribution for choosing the source and the terminal in a more

<sup>1</sup> From  $0.1N_t p_a + 0.9N_t p_n = R$  and  $p_a = 1000p_n$ , we derive the packet generation probabilities  $p_n = 1/1009$  and  $p_a = 1000/1009$  at a node per step.

realistic situation; packets are generated proportionally to a population in the territory of a node. By using a statistical population data on a geographical map, each mesh block (corresponding to a set of users) is assigned to the nearest access node (corresponding to a base station) in the sense of the Euclidean distance. The merged region by the assigned blocks to a node is its territory. Then, the population in the territory is defined by a sum of data at the assigned blocks. Figure 2 shows the cumulative population of nodes whose positions are uniformly at random for the initial setting of UDGs on a geographical map. Note that the density function of the population is nearly exponential, since the cumulative distribution is almost linear in a semi-log plot, and the derivative of an exponential function is also exponential. We confirm similar exponential-like distributions for several population data at other locations measured by the Japan Statistical Association. In such real data, it is common that big cities are located apart from each other while some nodes with high populations in their territories concentrate in and around a city. Thus, the selection of a node as the source or the terminal of a packet is proportional to the population in its territory under the normalization to be a probability distribution. For  $R$  packets per step, this process is repeated. We call it the packet generation according to the population. Although probabilistic selections of the source and the terminal are due to a general problem setting for the simulation, in practice, their nodes should be chosen by an objective determined beforehand. Therefore, it is natural for a user to know the position of a terminal without global information. This explanation supports a decentralized routing with only local information in the next subsection.

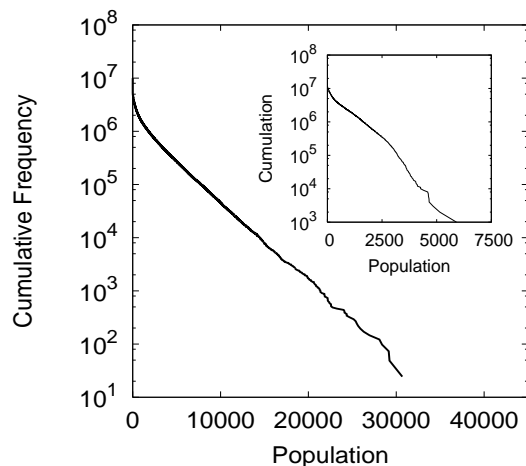


Fig. 2. Cumulative frequency of population in the territory of a node in UDGs over 50 realizations for  $N_0 = 1000$ . Inset shows the cumulation of population data in the original  $160 \times 160$  mesh blocks in  $80km^2$  (see Fig. 4 for the visualization). Both curves are nearly straight lines characterized as exponential distributions.

### 2.3 Routing protocol

Instead of the random walk [11,12], we consider a greedy routing [20] developed in computer science, as shown on the left of Fig. 3. It is also called a greedy searching or greedy forwarding algorithm. In order to forward a packet from the resident node  $u$  to a closer position to its terminal  $t$  in the sense of the Euclidean distance on a plane, a node  $v$  is chosen in the set  $\mathcal{N}_u$  of connecting one-hop neighbors of  $u$ , if the distance  $d_{vt}$  between nodes  $v$  and  $t$  is minimum:  $d_{vt} \leq d_{wt}$ ,  $v \neq w, \forall w \in \mathcal{N}_u$ , where ties for the minimum are broken randomly in  $\mathcal{N}_u$ . In this paper, the protocol is modified to that a packet is always transferred to a connecting neighbor  $v \in \mathcal{N}_u$  even if  $d_{vt} > d_{ut}$  (see the top right of Fig. 3). Moreover, to avoid falling into a trap of cycles, we apply the self-avoiding rule: a packet is not transferred to nodes that have already been visited (see the bottom right of Fig. 3), whose history is stored in memory. This deterministic routing can act with only local information (e.g. positions of one-hop neighbors measured by a GPS) even for any topological change including the mobility of nodes. Note that all existing packets independently move to one-hop neighbors by a one-time step. If a packet either arrives at its terminal or encounters a dead-end, it is removed.

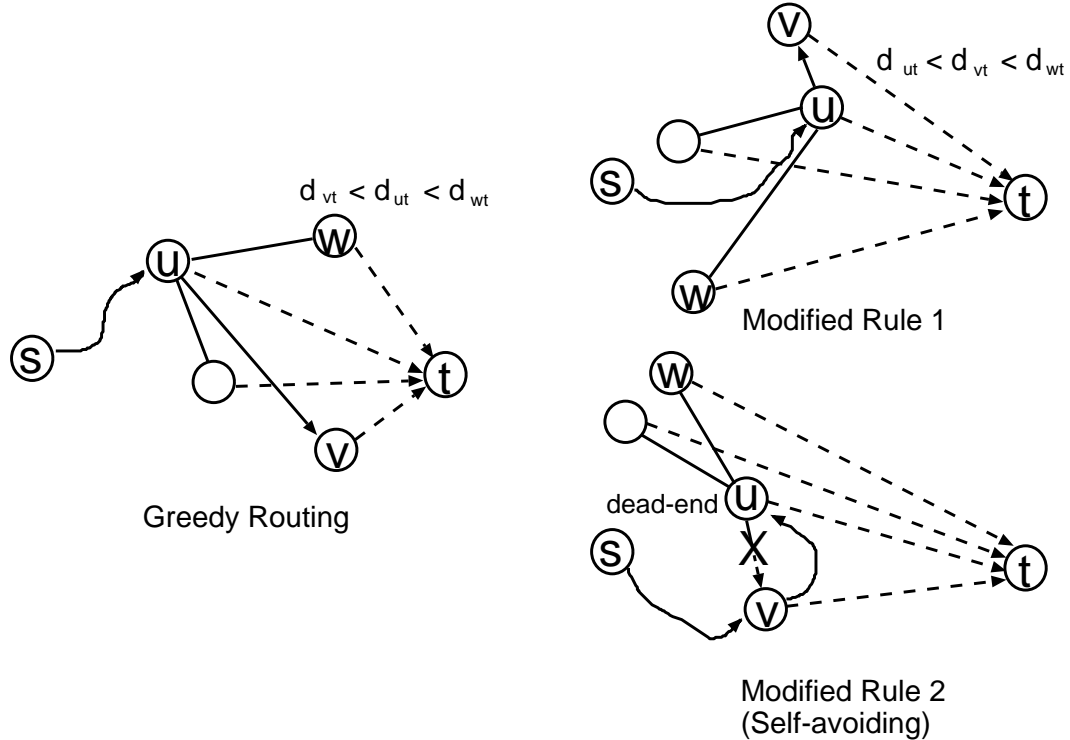


Fig. 3. Modified greedy routing. The solid straight line denotes a direct link to  $v$  or  $w$  in the set  $\mathcal{N}_u$  of connecting one-hop neighbors, and the dashed line denotes  $d_{vt}$  measured by the Euclidean distance from  $v \in \mathcal{N}_u$  to the terminal  $t$ . The curved line represents a path from the source  $s$  to the current resident node  $u$  of a packet.

## 2.4 Network self-organization

We propose the following efficient networks that are self-organized through two phases: the removal of links and the addition of shortcuts depending on traffic flows. Here, the simultaneous implementation of the two phases is outside the scope of this fundamental proposal, since the network generated by the simultaneous implementation destroys the initial structure of a UDG in a wireless environment and does not stably converge to a topological structure except with the trivial connections between active nodes. How to simultaneously implement them will be an issue.

First, we explain the base model for self-organization. In a **Link Survival(LS)** network, if a packet passes a link on the modified greedy routing, the weight is increased by 1. After the forwarding process for all packets, we check whether all link weights are decreased by 1 with probability  $p_d = 0.1$ . When the weight reaches 0 after the decreases chosen with  $p_d$  through several steps, then the link is removed, and isolated nodes without any links are also removed. From an initial UDG with size  $N_0$ , both the increase and the decrease of link weights are repeated until  $T = 3 \times 10^4$  steps in the steady state. The initial weights are set to 5 for all links in order not to be removed before packets reach them.

Next, we consider a **Path Reinforcement(PR)** network extended from the LS network by adding shortcuts. After stopping the removal of links at  $T$ , we continue the network generation and the transfer of packets to make 10 % or 30% of shortcuts for the total number of surviving links in the LS network. Each shortcut link is added between the current resident node of a randomly chosen packet and a randomly chosen node from the nodes that have already been visited on the routing path before arriving at its terminal. Such a direct shortcut between nodes separated by more than two hops suppresses the forming of a quasi-complete graph [11,12] in the hop-by-hop connections. To compare the communication efficiency and the robustness of connectivity with LS and PR networks, we further consider a **Random Shortcut(RS)** network. It is constructed by adding 10 % or 30% of shortcuts between two randomly chosen nodes independently from the positions of packets on the LS network. We emphasize that, in the previous studies for SF [21] and multi-scale quartered (MSQ) [22] networks, the robustness is significantly improved by adding such random shortcuts.

We do not discuss how to implement shortcut links in practice, since the problem will be solved by future wireless technologies, such as control of directivity and beam power, a hybrid network with wired links, etc. In addition, the values of  $p_d$  and  $T$  are set to be merely convenient for the simulation. For other values, we obtain results that are similar to those presented in the next section, provided that the value of  $p_d$  is not too large to maintain the connec-

tivity. Although almost all surviving links do not change any longer around  $1000 \sim 2000$  steps, we take sufficient time for  $T$ .

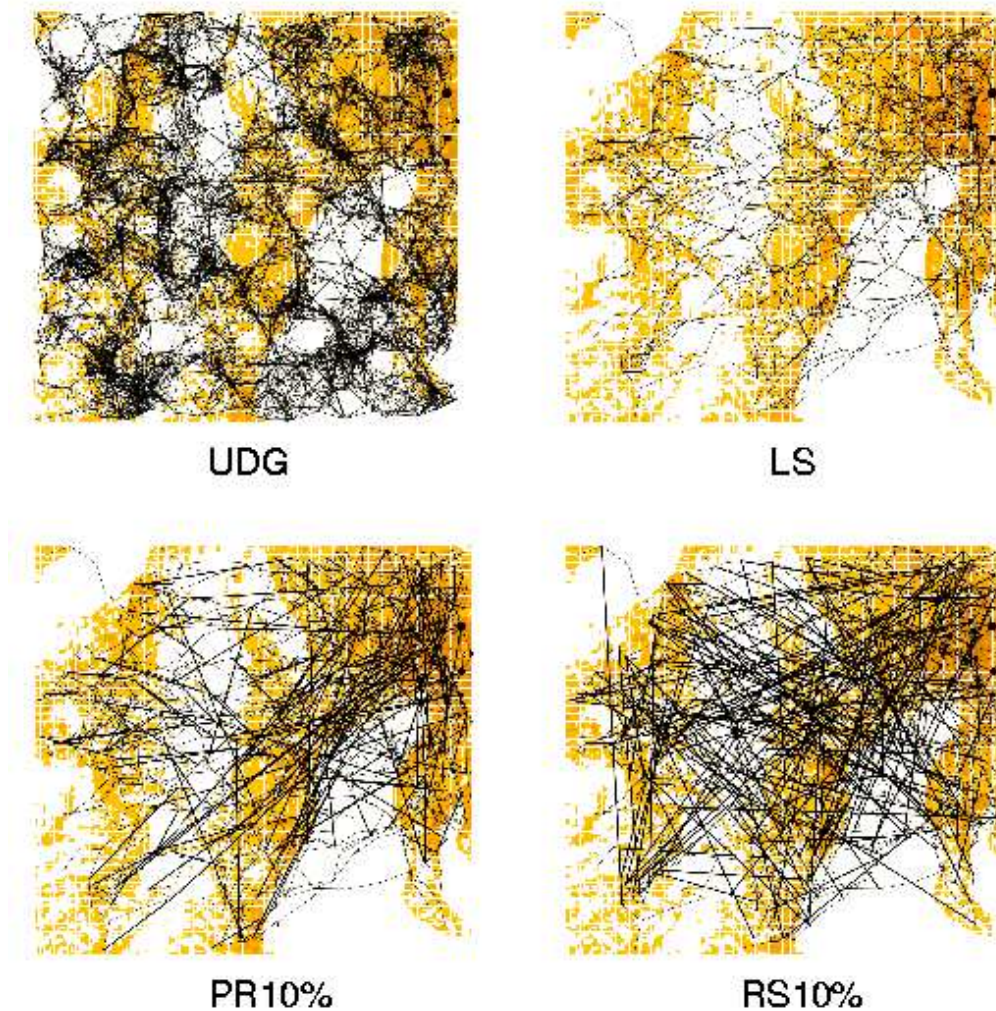


Fig. 4. (Color online) Visualization of the networks generated from a UDG with the initial size  $N_0 = 1000$ . In the LS, PR, and RS networks, the surviving nodes concentrate in high-population areas for which data is provided by the Japan Statistical Association. The gradation of mesh blocks from light to dark (white, yellow, orange, red) corresponds to the population density. The thick and thin lines are 10 % shortcuts and the other links in the LS network, respectively. The size of a black node is proportional to the population in its territory.

### 3 Efficiency and robustness

We investigate the topological structures of LS, PR, and RS networks. Here, the inclusion of graphs and the extension with shortcuts are  $UDG \supset LS \xrightarrow{\text{extension}} PR$  or  $RS$ , and the positions of nodes are identical in these networks except



for the removed parts. As shown in Fig. 4, an LS network is obtained from a UDG by removing some nodes in the (white) mountain or sea areas of low-population density, while the PR and RS networks have comparatively longer shortcuts between the areas of high-population density and between random positions, respectively. We remark that the LS network resembles a planar network without crossing links. The large black nodes correspond to active nodes with more packet generations. Surviving nodes naturally concentrate in dark (red) areas of large population similar to a router density map [23] in the real world. Here, the population in the territory of a removed node is reassigned to its neighboring nodes in the iterative process of network generation. Remember that the initial distribution of population assigned to a node in the UDG or to the original mesh in  $160 \times 160$  blocks decays exponentially (see Fig. 2). This exponential-like distribution of population is consistent for LS networks after surviving some nodes. In the following, we will focus on the results obtained for the packet generation according to the population. When the probability of packet generation at a node is set by  $p_a$  and  $p_n$  or by an exponential distribution  $\exp(-\gamma \times nid)$ , where  $\gamma > 0$  is a parameter and  $nid$  is an ID number:  $1, 2, \dots, N_0$  randomly assigned to a node in the UDG with no relation to its geographical position, there are no changes qualitatively.

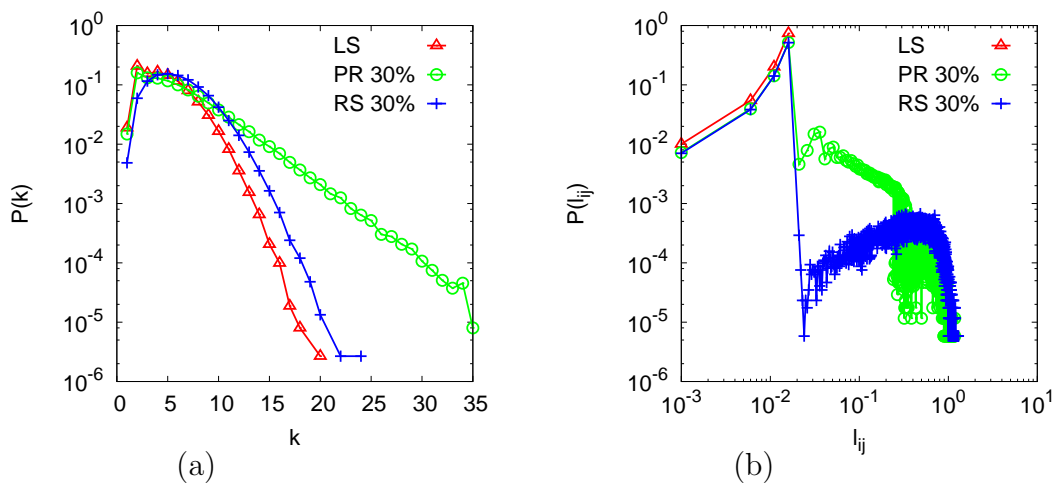


Fig. 5. (Color online) Distributions of (a) degree  $k$  and (b) link length  $l_{ij}$  in the networks generated from the initial size  $N_0 = 10000$ . (a) Bounded small degrees are held even with shortcuts. There exists no hub: the maximum degree is small as  $k_{max} \sim O(\log N_T)$ , since the tail indicates an exponential decay. (b) The right bottom parts marked by circle and plus signs denote longer shortcuts in PR and RS networks than the links in LS networks. Each plot is obtained by the average of 50 realizations.

As typical measures for the communication efficiency, we investigate the degrees and the link lengths. Because they are related to the costs for maintaining connections at a node and for constructing a link by wireless beam or wire cable, smaller values are suitable for the efficiency. The costs are usually evaluated by the maximum (in the worst case) and the average or the high-

Case	UDG	LS	PR10%	RS10%	PR30%	RS30%
Active-Normal	12.3	5.22	5.74	5.74	6.78	6.78
Population	12.3	4.56	5.01	5.01	5.92	5.92

Case	UDG	LS	PR10%	RS10%	PR30%	RS30%
Active-Normal	0.013	0.016	0.035	0.06	0.069	0.129
Population	0.013	0.016	0.033	0.058	0.065	0.123

Table 1

Average degree  $\langle k \rangle$  (top) and link length  $\langle l_{ij} \rangle$  (bottom) in the networks with active-normal nodes and the corresponding results for the packet generation according to the population. Each value is obtained by the average of 50 realizations generated from UDGs with the initial size  $N_0 = 10000$ .

$N_0$	100	200	500	1000	2000	5000	10000
Active-Normal	55.26	130.66	379.3	823.92	1728.56	4517.74	9180.98
Population	61.94	127.0	331.26	688.94	1425.4	3679.98	7489.92

Table 2

The number  $N_T$  of surviving nodes from the initial size  $N_0$  of UDGs. Note that the LS, PR, and RS networks have the same number of nodes.

frequency (in a standard case) values over a network. Figures 5(a)(b) show the distributions of degree and link length, and Table 1 shows their averages. The increasing order of  $\langle k \rangle$  is  $LS < PR \approx RS < UDG$ , and that of  $\langle l_{ij} \rangle$  is  $UDG < LS < PR < RS$ . In particular, RS networks have on average twice as long links than PR networks. It is a cause of the difference in  $\langle l_{ij} \rangle$  that the length of a shortcut is affected by the paths of packets in PR networks while it is determined only by the spatial distribution of surviving nodes which are embedded in RS networks. In addition, as shown in Fig. 5(b), PR networks are more efficient in the sense of link length by far than RS networks with no restriction on the link length except the scale of the area. On the whole, since the high-frequency parts of  $P(k)$  and  $P(l_{ij})$  consist of small values in spite of the effect of longer shortcuts added in the PR and RS networks, these networks are efficient with small degrees and short links.

As another measure of the efficiency, the average number of hops  $\langle L_{ij} \rangle$  on the shortest paths (measured by the minimum number of hops between two nodes) is important, because fewer hops are better for communicating through intermediate nodes as quickly as possible. It is useful to investigate the scaling behavior of  $\langle L_{ij} \rangle$  versus  $N_T$  for checking the small-world (SW) effect [24,25,26]. As shown in Fig. 6(a), the  $O(\sqrt{N_T})$  scaling in LS networks is improved to  $O(\log N_T)$  characterized as the SW effect in PR and RS networks with only 10-30 % of shortcuts. Surprisingly, this effect appears even in PR networks with

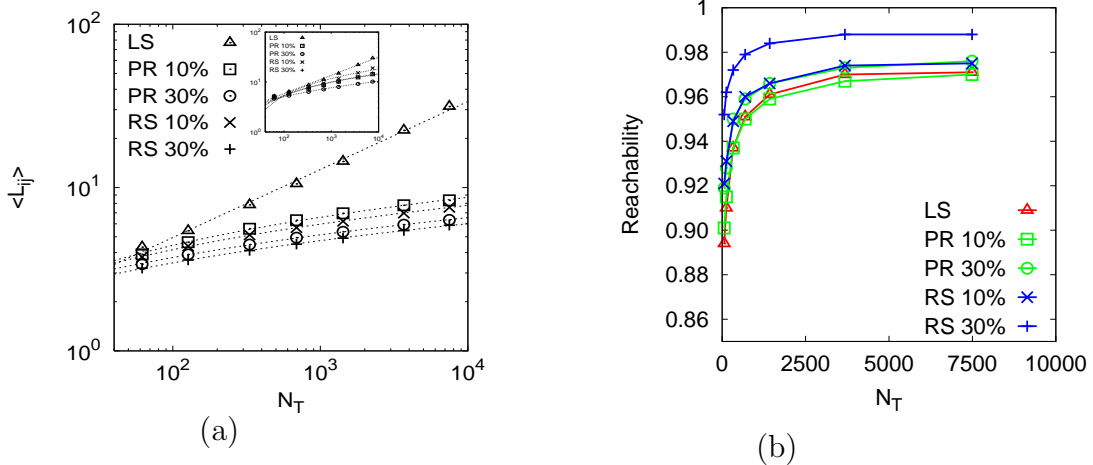


Fig. 6. (Color online) Routing properties. (a) The scaling behaviors of the average number  $\langle L_{ij} \rangle$  of hops on the shortest paths vs. the network size  $N_T$ . The estimated dashed lines are  $O(N_T^{0.42})$  in LS networks and  $O(\log N_T)$  as the SW effect in PR and RS networks with 10 % or 30 % shortcuts. The inset shows the similar scaling behavior for the modified greedy routing. (b) The high reachability for the modified greedy routing. Each plot is obtained from the average of 50 realizations.

more restricted shortcuts on the paths than in RS networks. Such change of scaling behaviors numerically occur within a transition of random-SW-regular phases [27], when the addition of long distance connections on a  $d$ -dimensional lattice is restricted by a probability  $P(l) \sim l^{-\delta}$  for the distance  $l$  with a control parameter  $\delta \geq 0$ . The related theoretical analysis is provided in [28]; however it is still open for more general cases beyond lattice structures. On the other hand,  $O(\sqrt{N_T})$  scaling usually appears in planar networks [14]. Table 2 shows the number  $N_T$  of surviving nodes from the initial size  $N_0$  of UDGs. The above improvement is also obtained for other paths on the modified greedy routing; however, the improvement becomes smaller as shown in the inset. Figure 6(b) shows the high reachability for the modified greedy routing in all of the networks. The reachability is defined by the fraction of packets successfully arriving at the terminals (they are not stopped at dead-ends) over all of the generated packets until  $T$  steps after constructing the networks.

We confirm the effect of shortcuts on the robustness against random failures and intentional attacks, in which nodes are removed at random and in decreasing order of degree before the removals, respectively. Figure 7 shows the relative size  $S/N$  of a giant component (GC) at  $N = N_T$  and the average size  $\langle s \rangle$  of the isolated clusters except the GC. The critical fraction of failures for the breaking of GC increases from 0.6 in LS networks to 0.8 in PR and RS networks with shortcuts. The critical fraction of attacks also increases from 0.4 in LS networks to around 0.6 in PR and RS networks. In comparison within similar average degrees, this robustness is at the same level in the optimal bimodal networks [29], and slightly stronger than that for Delaunay triangulations (DT) with  $\langle k \rangle \approx 6$  [21] and MSQ networks based on a

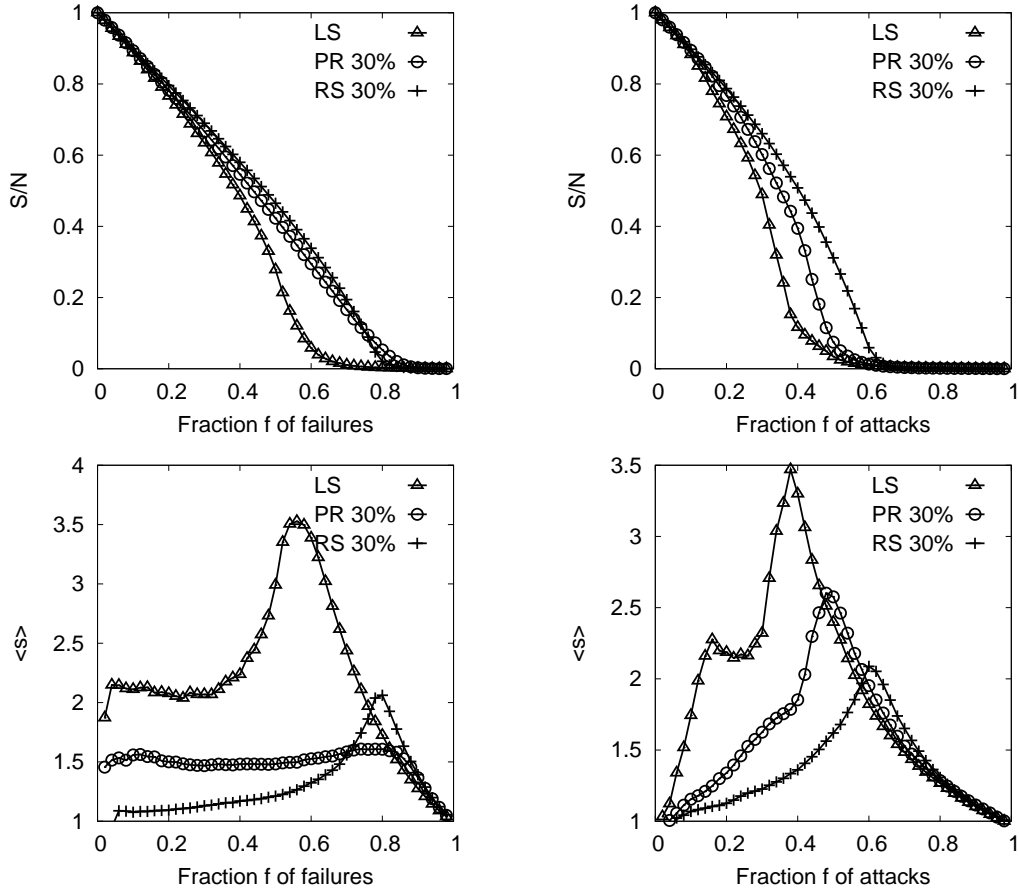


Fig. 7. Top: relative size  $S/N$  of the GC against random failures (left) and intentional attacks (right) in the networks generated from the initial size  $N_0 = 10000$ . Bottom: average size  $\langle s \rangle$  of isolated clusters except the GC. Note that the GC is broken at the relative maximum of  $\langle s \rangle$ , whose fraction yields the critical value. Each plot is obtained by the average of 50 realizations.

self-similar tiling [22] with  $\langle k \rangle = 4.54$ . Remember that [13] a GC is broken by attacking only a few percent of hubs in SF networks. In addition, the interesting problem is whether the percolation transition exists or not in our self-organized networks. Especially, the critical point of  $\langle s \rangle$  is indistinct for random failures in the PR networks marked by circles at the bottom left of Fig. 7 in the cases of packet generation according to the population (also for other data); however the divergence peak appears in the cases of an artificially defined probability distribution for packet generation as shown in Fig. 8. We will further investigate the reason why the difference occurs.

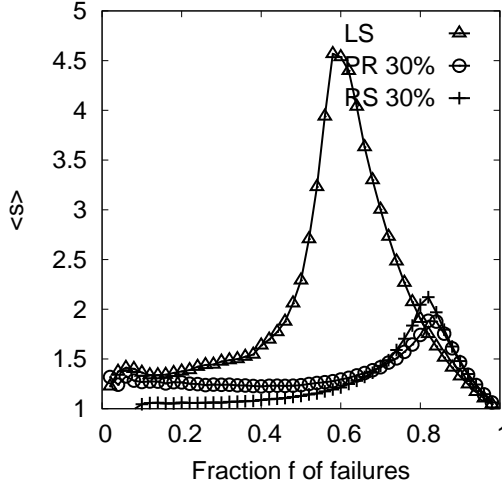


Fig. 8. Suggestion of percolation transition. The divergence peak appears when the probability of packet generation at a node is artificially set by  $p_a$  and  $p_n$  or by an exponential distribution with no relation to its geographical position.

#### 4 Conclusion

In summary, we propose self-organized geographical networks by link survival and addition of shortcuts according to packet flows on decentralized routing in a wireless environment. We show that the positions of surviving nodes naturally concentrate on the areas of high-population density, and that the links between them are short. By adding only 10-30 % shortcuts, the average number of hops on the routing paths is improved from  $O(\sqrt{N_T})$  in LS networks to  $O(\log N_T)$  as the SW effect [24,25,26]. Moreover, for both random failures and intentional attacks, the robustness of connectivity increases to reach the same level as in the optimal bimodal networks [29]. The uniformly random shortcuts are slightly better for the robustness than the ones by the path reinforcement. Probably, random shortcuts tend to be useful for a strong robustness by bridging distributed local areas; however the optimal shortcuts are an open problem. Thus, our self-organized networks with shortcuts keep a high communication efficiency in SF networks, but also overcome their vulnerability [13]. For other criteria, e.g. maximizing the end-to-end throughput [17], it is an attractive issue to find the optimal network structure and the self-organization mechanism. Various network formations by other weight update rules and routings will be also further investigated for future communication infrastructures, smart grids, and urban planning.

## Acknowledgment

The authors would like to thank the anonymous reviewers for their valuable comments to improve both insufficient descriptions and the readability of the manuscript. This research is supported in part by a Grant-in-Aid for Scientific Research in Japan, No. 21500072.

## References

- [1] A. Tero, S. Takagi, T. Saigusa, K. Ito, D.P. Bebbler, M.D. Fricker, K. Yumiki, R. Kobayashi, and T. Nakagaki, *Science* **327**, 439, (2010).
- [2] A. Runions, A.M. Fuhrer, B. Lane, P. Federl, A.-G. Rolland-Largan, and P. Prusinkiewicz, *ACM Transactions on Graphics* **24(3)**, 702-711, (2005).
- [3] A.F.M. Marée, and P. Hogeweg, *PNAS* **98(7)**, 3879, (2001).
- [4] A.F.M. Marée, and P. Hogeweg, *Bulletin of Math. Bio.* **64**, 327-353, (2002).
- [5] D. Helbing, J. Keltsch, and P. Molnár, *Nature* **388**, 47, (1997).
- [6] F. Xie, and D. Levinson, *Transport. Res. Part E* **44**, 100, (2008).
- [7] P. Holme, and M.E.J. Newman, *Phys. Rev. E* **74**, 056108, (2006).
- [8] S. Gil, and H. Zanette, *Physica A* **356**, 89, (2006).
- [9] S.-W. Kim, and J.D. Noh, *Phys. Rev. Lett.* **100**, 118702, (2008).
- [10] S.-W. Kim, and J.D. Noh, *Phys. Rev. E* **80**, 026119, (2009).
- [11] N. Ikeda, *Physica A* **379**, 701, (2007).
- [12] N. Ikeda, *J. Phys. A: Math. Theor.* **41**, 235005, (2008).
- [13] R. Albert, H. Jeong, and A.-L. Barabási, *Nature* **406**, 379, (2000).
- [14] M. Barthélemy, and A. Flammini, *Phys. Rev. Lett.* **100**, 138702, (2008).
- [15] Q. Xuan, F. Du, and T.-J. Wu *Phys. Rev. E* **82**, 046116, (2010).
- [16] M.A. Rajan, M. Grish Chandra, Lokanatha Reddy, and Prakash Hiremath *Int. J. of Computers, Communications & Control*, ISSN:1841-9836, *Proc. of the ICCCC*, pp.465-469, (2008).
- [17] W. Krause, J. Scholz, and M. Greiner, *Physica A.* **361**, 707, (2006).
- [18] J. Dall, and M. Christensen, *Phys. Rev. E* **66**, 016121, (2002).
- [19] F.A. Onat, and I. Stojmenovic, *Pervasive and Mobile Computing* **4**, 597-615, (2008).

- [20] K.-W. Fan, S. Liu, and P. Sinha, Ad Hoc Routing Protocols, In *Handbook of Algorithms for Wireless Networking and Mobile Computing*, edited by A. Boukerche, (Chapman & Hall/CRC, 2006), Chap. 9.
- [21] Y. Hayashi, and J. Matsukubo, *Physica A* **380**, 552, (2007).
- [22] Y. Hayashi, *Physica A* **388**, 991, (2009).
- [23] S.-H. Yook, H. Jeong, and A.-L. Barabási, *PNAS* **99(21)**, 13382, (2002).
- [24] D.J. Watts, and S.H. Strogatz, *Nature* **393**, 440, (1998).
- [25] R. Albert, H. Jeong, and A.-L. Barabási, *Nature* **401**, 130, (1999).
- [26] M. Barthélemy, and L.A. Amaral, *Phys. Rev. Lett.* **82**, 3180, (1999).
- [27] P. Sen, K. Banerjee, and T. Biswas, *Phys. Rev. E* **66**, 037102, (2002).
- [28] J.Kleinberg, *Nature*, **406**, 845, (2000). *Proc. 32nd ACM Symposium on Theory of Computing, 2000*. Cornell Computer Science Technical Report 99-1776 (October 1999). <http://www.cs.cornell.edu/home/kleinber/swn.pdf>
- [29] T. Tanizawa, G. Paul, S. Havlin, and H.E. Stanley, *Phys. Rev. E* **74**, 016125, (2006).